The Use of Homotopy Analysis Method to Solve the Time-Dependent Nonlinear Eikonal Partial Differential Equation

Mehdi Dehghan and Rezvan Salehi

Department of Applied Mathematics, Faculty of Mathematics and Computer Science, Amirkabir University of Technology, No. 424, Hafez Ave., 15914, Tehran, Iran

Reprint requests to M. D.; E-mail: mdehghan@aut.ac.ir, mdehghan.aut@gmail.com or R. S.; E-mail: rezvansalehi@aut.ac.ir

Z. Naturforsch. **66a,** 259 – 271 (2011); received April 8, 2010 / revised July 21, 2010

In this research work a time-dependent partial differential equation which has several important applications in science and engineering is investigated and a method is proposed to find its solution. In the current paper, the homotopy analysis method (HAM) is developed to solve the eikonal equation. The homotopy analysis method is one of the most effective methods to obtain series solution. HAM contains the auxiliary parameter $\hbar$, which provides us with a simple way to adjust and control the convergence region of a series solution. Furthermore, this method does not require any discretization, linearization or small perturbation and therefore reduces the numerical computation a lot. Some test problems are given to demonstrate the validity and applicability of the presented technique.

Key words: Homotopy Analysis Method; Eikonal Equation; Semi-Analytic Approaches; Time-Dependent Partial Differential Equations; Applications; Adomian Decomposition Method; Hamilton-Jacobi Equation.
AMS subject classifications: 74G10, 35C10, 70H20

1. Introduction

The Hamilton-Jacobi time-dependent partial differential equation,

$$\psi_t + H(x, \nabla \psi(x,t)) = 0, \tag{1}$$

arises in many applications ranging from classical mechanics to contemporary problems of optimal control. These include geometrical optics, crystal growth, etching, computer vision, obstacle navigation, path planning, photolithography, and seismology.

A very important member of the family of the static Hamilton-Jacobi equations is the eikonal equation. The stationary eikonal equation is

$$|\nabla u(x)| = \eta(x), \quad x \in \mathbb{R}^n, \tag{2}$$

with a boundary condition $u(x) = \phi(x)$, $x \in \Gamma \subset \mathbb{R}^n$. The eikonal equation has many applications in optimal control [1, 2], computer vision [3 – 5], geometric optics [6], path planning [7, 8], etc. The equation is closely related to conservation laws, and information travels with characteristics or rays from the boundary. If $\eta = 1$ and $\phi = 0$ then the solution $u(x)$ is the distance between the point x and the boundary. If η depends on x, $u(x)$ is the phase of high frequency wave travelling in a medium with variable speed of propagation.

Two different type of methods can be found to solve the eikonal equation. One approach is to treat the problem as a static (time-independent) boundary value problem and design an efficient numerical algorithm to solve the system of nonlinear equations after discretization. For example, the fast marching [9, 10] and fast sweeping methods [11, 12] are of these types. The fast marching method employs a heap to sort points on the moving wavefront. This is based on the property of the solution that guarantees the characteristic steepest descent on u. The solution at each point depends on points with smaller values, and updating the minimum value on the wavefront, using the heap-sort maintains this condition. The complexity of this algorithm is of order $O(N \log N)$ for N grid points, where the $\log N$ factor comes from the heap-sort algorithm. On the other hand, one can update solutions along a specific direction without explicit checks for causality property. This is the main idea behind the fast sweeping method which solves the problem on an n-dimensional grid using at least 2^n directional sweeps, one per quadrant, within a Gauss-Seidel update scheme. The fast sweeping is optimal in the sense that a finite number of

iterations is needed [12], so that the complexity of the algorithm is $O(N)$ for a total number of N grid points, although the constant in the complexity depends on the equation.

The high-order finite difference type fast sweeping method developed in [11] provides a quite general framework, and it is easy to incorporate any order of accuracy and any type of numerical Hamiltonian into the framework. Much faster convergence speed than that by the time-marching approach can be achieved. Several other numerical schemes are extended to solve Hamilton-Jacobi equations for example the essentially non-oscillatory (ENO) scheme [13], the weighted ENO (WENO) scheme [14], the discontinuous Galerkin method [15], etc.

The other class of numerical methods for static Hamilton-Jacobi (HJ) equations is based on the reformulation of the equations into suitable time-dependent problems. One technique to obtain a time-dependent Hamilton-Jacobi equation is using the so called paraxial formulation [13, 16 – 18]. Another approach is the level set method. A large number of applications require the development of optimal algorithms for tracking moving interfaces (that is, advancing fronts). Advances in numerical analysis have led to computationally efficient tools for tracking interface motion by using level set methods. The level set method first introduced by Osher and Sethian [19] in 1988 is a simple and adaptable method for computing and analyzing the motion of an interface in two or three dimensions and following the evolution of interfaces [20]. The main idea of the level set method is to embed the propagating interface as the zero level set of a continuous real valued function, called a level set function. Let φ denote this function then φ embeds the interface Γ as its zero level set $\Gamma(t=0)=\{x\in\mathbb{R}^n \mid \varphi(x)=0\}$. Furthermore, by adding a time variable, the level set function can be used to capture a given dynamics of the interface using a time dependent partial differential equation (PDE) in φ. The location of the interface at time t in this case is the zero level set of φ at that time: $\Gamma(t)=\{x\in\mathbb{R}^n \mid \varphi(x,t)=0\}$.

Osher [21] provided a link to the time dependent Hamilton-Jacobi equations by proving that the t-level set of $\varphi(x,y)$ is the zero level set of the viscosity solution of the evolution equation at time t. In that paper, Osher derived from the general first-order equation

$$\mathcal{F}(x,y,u,u_x,u_y)=0 \tag{3}$$

a time-dependent Hamilton-Jacobi equation,

$$\varphi_t+H(x,y,t,\varphi_x,\varphi_y)=0, \tag{4}$$

on domain $\Omega\subseteq\mathbb{R}^n$ and subject to initial conditions $\varphi(x,t=0)=\varphi_0(x)$ for $x\in\Gamma\subset\partial\Omega$. Osher and Sethian developed a Hamilton-Jacobi scheme with second-order viscosity for a curve propagation with curvature-dependent speed. In that work, they considered a small section of curve $t=u(X)$, as u is satisfied in the eikonal equation, and produced an evolution equation of the form

$$\Psi_t+F(K)(1+|\nabla\Psi|^2)^{1/2}=G(X,\nabla\Psi,\varepsilon),\ X\in\mathbb{R}^d, \tag{5}$$

where $x_d=\Psi(x_1,\ldots,x_{d-1},t)$ and K is the curvature. At the same time, if we view the curve $t=u(X)$ as a level set of the function $\Phi(X,t)=C$, we are led to the Hamilton-Jacobi equation

$$\Phi_t+c(X)|\nabla\Phi|=0,\quad X\in\mathbb{R}^d. \tag{6}$$

2. The Main Problem

In this paper, we consider the time-dependent eikonal equations (7) and (8) that are formulated by the aid of the level set method. According to the level set framework, if we view the curve $t=u(x)$ as a level set of the function $\phi(x,t)=c$, we are led to the Hamilton-Jacobi equation

$$\phi_t(x,t)+c(x)|\nabla\phi(x,t)|=0,\ \text{ in }\ \Omega\times[0,T]. \tag{7}$$

At the same time, if considering a small section of curve $t=u(X)$, as u is satisfied in (2), then we can produce an evolution equation of the form

$$\psi_t+f(X)(1+|\nabla\psi|^2)^{1/2}=0,\ \text{ in }\ \Omega\times[0,T], \tag{8}$$

where $x_d=\psi(x_1,\cdots,x_{d-1},t)$, $d=2$, 3, and subject to the initial conditions

$$\phi(x,t_0)=g(x),\quad \psi(X,t_0)=h(X),\quad x\in\Omega, \tag{9}$$

where $c(x)=\frac{1}{\eta(x)}$, $g(x)$ and $h(x)$ are Lipschitz continuous functions.

In this investigation, we focus on an eikonal equation which is transformed in the form of a Hamilton-Jacobi equation by the level set formulation. These equations are solved numerically by several authors. Interested reader can see [16, 22] and the references

therein. But the current paper proposes a different approach. The main idea behind this work is to use a semi-analytic (or quasi-numerical) technique [23]. The solution is given by means of the homotopy analysis method (HAM). Several examples are given to show the efficiency of this method for solving the studied model.

The rest of this paper is arranged as follows: In Section 3, we present the mathematical framework of the homotopy analysis method. In Section 4, several test problems are given, and results obtained by the presented method are reported. In Section 5, some applications of this model are prescribed. Section 6 completes this paper with a brief conclusion.

3. The Homotopy Analysis Method

The homotopy analysis method (HAM) has been proposed by S. J. Liao in his Ph. D. dissertation in 1992. In [24], Liao employed the basic idea of the homotopy in topology to propose a general analytic method for nonlinear problems. Based on homotopy of topology, the validity of the HAM is independent of whether or not there exist small parameters in the considered equation. Therefore, the HAM can overcome the foregoing restrictions and limitations of perturbation techniques. The HAM also avoids discretization and provides an efficient numerical solution with high accuracy and minimal calculation. Furthermore, the HAM always provides us with a family of solution expressions in the auxiliary parameter $\hbar$ [25], the convergence region might be determined conveniently by the auxiliary parameter $\hbar$.

Several authors have used HAM to solve various problems in applied mathematics. This technique is used in [26] for solving Blasius' viscous flow which is the two-dimensional laminar viscous flow over a semi-infinite flat plate. In [27] this method is applied to give an analytic solution of the viscous flow past a sphere. In [28] HAM is used to solve the combined heat and mass transfer by natural convection adjacent to a vertical wall in a non-Darcy porous medium. In [29] HAM is applied to find the exact flow of a third-grade fluid past a porous plate. In addition, this method is applied in [30] for solving the time fractional wave-like differential equation with a variable coefficient. This method is applied in [31] to solve the Thomas-Fermi equation. This technique is used for computing a solitary wave solution of the modified Camassa-Holm equation in [32]. Author of [33] implemented the HAM for solving the Laplace equation with Dirichlet and Neumann boundary conditions. This technique is also applied in [34] to compute an explicit series solution of travelling waves with a front of the Fisher equation. In [35] the heat transfer analysis is investigated for magnetohydrodynamic (MHD) flow in a porous channel, and the homotopy analysis method is employed to obtain the expressions for velocity and temperature fields. Authors of [36] presented an efficient numerical algorithm for solving the nonlinear algebraic equations based on the Newton-Raphson method and HAM. The higher-dimensional initial boundary value problems of variable coefficients are solved by means of HAM [37]. In [38] the problem of a magnetohydrodynamic boundary layer flow of an upper-convected Maxwell (UCM) fluid is considered for the analytical solution using HAM. Authors of [39] introduced a reliable modification of HAM and applied it to homogeneous or non-homogeneous differential equations with constant or variable coefficients. They assumed that the 'coefficients' and/or non-homogeneous terms can be expressed in Taylor series based on a kind of a continuous homotopy mapping with respect to p (embedding parameter). For more applications of HAM the interested reader can see [40 – 45]. Beyond that for some other semi-analytical approaches the reader can see [46 – 52].

3.1. Basic Idea of HAM

To illustrate the basic idea of the homotopy analysis method, let us consider the following differential equation:

$$\mathcal{N}[u(r)] = 0, \tag{10}$$

where $\mathcal{N}$ is a nonlinear operator, r denotes the independent variable, and $u(r)$ is an unknown function. By means of generalizing the traditional homotopy method, Liao constructs the so-called zero-order deformation equation

$$(1-p)\mathcal{L}[\phi(r;p) - u_0(r)] = p\hbar H(r)\mathcal{N}[\phi(r;p)], \tag{11}$$

where $p \in [0,1]$ is the embedding parameter, $\hbar \neq 0$ is a non-zero auxiliary parameter, $H(r) \neq 0$ is an auxiliary function, $\mathcal{L}$ is an auxiliary linear operator, $u_0(r)$ is an initial guess of $u(r)$, and $u(r;p)$ is an unknown function. Expanding $u(r;p)$ in Taylor series with respect to p, we have

$$\phi(r;p) = u_0(r) + \sum_{m=1}^{\infty} p^m u_m(r), \tag{12}$$

where

$$u_m(r) = \frac{1}{m!}\frac{\partial^m \phi(r;p)}{\partial p^m}|_{p=0}. \quad (13)$$

If the auxiliary linear operator, the initial guess, the auxiliary parameter $\hbar$, and the auxiliary function are so properly chosen, the series (12) converges at $p = 1$, then we have

$$u(r) = u_0(r) + \sum_{m=1}^{\infty} u_m(r), \quad (14)$$

which must be one solution of the original nonlinear equation. As $\hbar = -1$ and $H(r) = 1$, (11) becomes

$$(1-p)\mathcal{L}[\phi(r;p) - u_0(r)] + p\mathcal{N}[\phi(r;p)] = 0. \quad (15)$$

Define the vector

$$\vec{u}_n(r) = \{u_0(r), u_1(r), \ldots, u_n(r)\}. \quad (16)$$

Differentiating (11) m times with respect to the embedding parameter p and then setting $p = 0$ and finally dividing them by $m!$, we have the so-called mth-order deformation equation

$$\mathcal{L}[u_m(r) - \chi_m u_{m-1}(r)] = \hbar H(r)\mathcal{R}_m(\vec{u}_{m-1}), \quad (17)$$

where

$$\mathcal{R}_m(\vec{u}_{m-1}) = \frac{1}{(m-1)!}\frac{\partial^{m-1}\mathcal{N}[\phi(r;p)]}{\partial p^{m-1}}|_{p=0} \quad (18)$$

and

$$\chi_m = \begin{cases} 0, & m \le 1, \\ 1, & m > 1. \end{cases}$$

By Theorem 2.1 in [53], (18) can be reformulated in the following form:

$$\mathcal{R}_m(\vec{u}_{m-1}) = \frac{1}{(m-1)!}\frac{\partial^{m-1}\mathcal{N}\left[\sum_{k=0}^{m-1} p^k u_k\right]}{\partial p^{m-1}}|_{p=0}. \quad (19)$$

It should be emphasized that $u_m(r)$ for $m \ge 1$ is governed by the linear equation (17) with the linear boundary conditions that come from the original problem, which can be easily solved by the well-known symbolic computation softwares such as Maple, Mathematica or Macsyma.

4. Test Problems

In this section, we present some examples with analytic solutions for the validation of HAM. Most of the test problems presented here are taken from the literature on high-order methods for hyperbolic problems: discontinuous Galerkin finite element method [54, 55], viscosity solutions approach [5], level set method [20, 56].

4.1. Example 1

As the first example, we consider the following initial value problem:

$$u_t(x,t) + |u_x(x,t)| = 0 \quad (20)$$

with the initial condition

$$u(x,0) = \min\{x, -2(x-2)\}. \quad (21)$$

For application of the homotopy analysis method, we choose the initial condition

$$\begin{aligned} u_0(x,t) &= u(x,0) \\ &= \min\{x, -2(x-2)\} \end{aligned} \quad (22)$$

and choose the linear operator

$$\mathcal{L}[\phi(x,t;p)] = \frac{\partial \phi(x,t;p)}{\partial t} \quad (23)$$

with the property

$$\mathcal{L}(c) = 0, \quad (24)$$

where c is the integral constant. Furthermore, from (20) we suggest to define the nonlinear operator

$$\mathcal{N}[\phi(x,t;p)] = \phi_t(x,t;p) + |\phi_x(x,t;p)|. \quad (25)$$

As simplest initial approximation for $u(x,t)$ we choose $u \equiv u_0 = u(x,0)$. It is immediately obvious that $u_0 = u(x,0)$ satisfies the initial condition automatically. Using the above definition, with assumption $H(x,t) = 1$, the zeroth-order deformation equation and the corresponding initial condition has the form

$$\begin{aligned} &(1-p)\mathcal{L}[\phi(x,t;p) - u_0(x,0)] \\ &\quad = p\hbar\mathcal{N}(\phi(x,t;p)), \end{aligned} \quad (26)$$

subject to the initial condition

$$\phi(x,0,p) = u(x,0). \quad (27)$$

It easily can be seen that for $p=0$, (25)–(27) lead to the relationship

$$\phi(x,t;0)=u_0(x,t). \tag{28}$$

Therefore, as embedding parameter p increases from 0 to 1, $\phi(x,t;p)$ varies from initial condition $u_0(x)$ to the solution $u(x,t)$. Expanding $\phi(x,t;p)$ in Taylor's series with respect to p, one has

$$\phi(x,t;p)=u_0(x,t)+\sum_{m=1}^{\infty}p^m u_m(x,t), \tag{29}$$

where

$$u_m(x,t)=\frac{1}{m!}\frac{\partial^m\phi(x,t;p)}{\partial p^m}|_{p=0}. \tag{30}$$

Define the vector

$$\vec{u}_n(x,t)=\{u_0(x,t),u_1(x,t),\ldots,u_n(x,t)\}. \tag{31}$$

Differentiating the zero-order deformation equation (26) m times with respect to p and finally dividing by $m!$, we gain the mth-order deformation equation

$$\mathcal{L}[u_m(x,t)-\chi_m u_{m-1}(x,t)]=\hbar\mathcal{R}_m(\vec{u}_{m-1}), \tag{32}$$

subject to the initial condition

$$u_m(0,0)=0, \tag{33}$$

where

$$\mathcal{R}_m(\vec{u}_{m-1})=\frac{1}{(m-1)!}\frac{\partial^{m-1}\mathcal{N}[\phi(x,t;p)]}{\partial p^{m-1}}|_{p=0} \tag{34}$$

$$=\frac{1}{(m-1)!}\frac{\partial^{m-1}\left[\sum_{k=0}^{m-1}p^k(u_k)_t+\left|\sum_{k=0}^{m-1}p^k(u_k)_x\right|\right]}{\partial p^{m-1}}|_{p=0} \tag{35}$$

and

$$\chi_m=\begin{cases}0, & m\le 1,\\ 1, & m>1.\end{cases} \tag{36}$$

Now the solution of the mth-order deformation equation (32) for $m\ge 1$ becomes

$$u_m(x,t)=\chi_m u_{m-1}(x,t)+\hbar\mathcal{L}^{-1}[\mathcal{R}_m(\vec{u}_{m-1})]+c_1. \tag{37}$$

According to the initial condition (22), we have $u_m(0,0)=0$, this implies that the integration constant c_1 occurring in (37) is zero. From (22) and (37), we now successively obtain

$$u_0(x,t)=\min\{x,-2(x-2)\}$$
$$=\begin{cases}x; & \text{if } x<\frac{4}{3},\\ -2(x-2), & \text{if } x>\frac{4}{3},\end{cases}$$

$$(u_0)_x(x,t)=\begin{cases}1, & \text{if } x<\frac{4}{3},\\ -2, & \text{if } x>\frac{4}{3},\end{cases}$$

$$|(u_0)_x(x,t)|=\begin{cases}1, & \text{if } x<\frac{4}{3},\\ 2, & \text{if } x>\frac{4}{3},\end{cases}$$

$$u_1(x,t)=\hbar\mathcal{L}^{-1}[\mathcal{R}_1(\vec{u}_0)]=\hbar\mathcal{L}^{-1}[(u_0)_t+|(u_0)_x|]$$
$$=\hbar\mathcal{L}^{-1}\cdot\begin{cases}1\\2\end{cases}=\begin{cases}\hbar t, & \text{if } x<\frac{4}{3},\\ 2\hbar t, & \text{if } x>\frac{4}{3},\end{cases}$$

$$(u_1(x,t))_x=0,$$

$$u_2(x,t)=u_1+\hbar\mathcal{L}^{-1}[\mathcal{R}_2(\vec{u}_1)]$$
$$=u_0+\hbar\mathcal{L}^{-1}\frac{\partial[(u_0+pu_1)_t+|(u_0+pu_1)_x|]}{\partial p}\Big|_{p=0}$$
$$=(1+\hbar)u_1(x,t),$$

$$u_3(x,t)=u_2+\hbar\mathcal{L}^{-1}[\mathcal{R}_3(\vec{u}_2)]=u_2+\hbar\mathcal{L}^{-1}$$
$$\cdot\frac{\partial^2\left[(u_0+pu_1+p^2u_2)_t+|(u_0+pu_1+p^2u_2)_x|\right]}{\partial p^2}\Big|_{p=0}$$
$$=(1+\hbar)^2u_1(x,t),$$
$$\vdots$$

At last, we get

$$(u_n(x,t))_x=0,\quad \forall n\ge 1,$$

$$\mathcal{R}_n(\vec{u}_{n-1})=$$
$$\frac{\partial^{n-1}\left[\left(\sum_{k=0}^{n-1}p^ku_k\right)_t+\left|\left(\sum_{k=0}^{n-1}p^ku_k\right)_x\right|\right]}{\partial p^{n-1}}\Big|_{p=0}$$
$$=\frac{\partial^{n-1}\left[\sum_{k=0}^{n-1}p^k(u_k)_t+|(u_0)_x|\right]}{\partial p^{n-1}}\Big|_{p=0}=(u_{n-1})_t,$$
$\forall n\ge 2,$

$$u_n(x,t)=u_{n-1}+\hbar\mathcal{L}^{-1}[\mathcal{R}_n(\vec{u}_{n-1})]$$
$$=(1+\hbar)^{n-1}u_1(x,t),\quad \forall n\ge 2.$$

The solution of (20) in the series form can be given by

$$u(x,t)=u_0(x,t)+\hbar u_1(x,t)+u_1(x,t)\sum_{k=1}^{\infty}(1+\hbar)^k. \quad (38)$$

Note that the coefficients of the solution expression (38) depend upon the auxiliary parameter $\hbar$. According to the convergence condition for geometric series, the necessary condition for the series (38) to be convergent is $|1+\hbar|<1$, i. e.,

$$-2<\hbar<0.$$

By setting $\hbar=-1$ in the above series solution, we obtain

$$\begin{aligned}u(x,t)&=u_0(x,t)-u_1(x,t)\\&=\min\{x-t,-2(x-2)-2t\},\end{aligned}$$

which is the exact solution of (20).

4.2. Example 2

Consider the equation

$$u_t(x,t)+|u_x(x,t)|=0 \quad (39)$$

and the initial condition

$$u(x,0)=\sin(x). \quad (40)$$

According to HAM, we choose the initial approximation

$$u_0(x,t)=u(x,0)=\sin(x) \quad (41)$$

and the linear operator

$$\mathcal{L}[\phi(x,t;p)]=\frac{\partial\phi(x,t;p)}{\partial t} \quad (42)$$

with the property

$$\mathcal{L}(c)=0, \quad (43)$$

where c is the integral constant. Furthermore, (39) suggests to define the nonlinear operator

$$\mathcal{N}[\phi(x,t;p)]=\phi_t(x,t;p)+|\phi_x(x,t;p)|. \quad (44)$$

Using the above definition with the assumption $H(x,t)=1$, we construct the zeroth-order deformation equation

$$(1-p)\mathcal{L}[\phi(x,t;p)-u_0(x,0)]=p\hbar\mathcal{N}(\phi(x,t;p)). \quad (45)$$

As mentioned previously in Example 1, for $p=0$, we get

$$\phi(x,t;0)=u_0(x,t). \quad (46)$$

The mth-order deformation equation is

$$\mathcal{L}[u_m(x,t)-\chi_m u_{m-1}(x,t)]=\hbar\mathcal{R}_m(\vec{u}_{m-1}), \quad (47)$$

subject to the initial condition

$$u_m(0,0)=0, \quad (48)$$

where

$$\mathcal{R}_m(\vec{u}_{m-1})=\frac{1}{(m-1)!}\frac{\partial^{m-1}\mathcal{N}[\phi(x,t;p)]}{\partial p^{m-1}}|_{p=0} \quad (49)$$

and

$$\chi_m=\begin{cases}0, & m\le 1,\\ 1, & m>1.\end{cases}$$

Now the solution of mth-order deformation equation (47) for $m\ge 1$ becomes

$$u_m(x,t)=\chi_m u_{m-1}(x,t)+\hbar\mathcal{L}^{-1}[\mathcal{R}_m(\vec{u}_{m-1})]+c_1. \quad (50)$$

From the initial condition (40), we conclude that $u_m(0,0)=0$ which yields the integration coefficient c_1 is zero. We now successively obtain

$$\begin{aligned}&u_0(x,t)=\sin(x),\\&u_1(x,t)=\hbar t\,|\cos(x)|,\\&u_2(x,t)=(1+\hbar)u_1(x,t)-\frac{t^2\hbar^2}{2!}\sin(x),\\&u_3(x,t)=(1+\hbar)u_2(x,t)\\&\qquad+\frac{\hbar^3t^3}{3!}\,\mathrm{abs}(1,-\cos(x))\cos(x)\\&\qquad+\frac{(1+\hbar)\hbar t^2}{2!}\,\mathrm{abs}(1,\cos(x))\sin(x),\\&\vdots\end{aligned}$$

Thus the HAM series solution of the initial value problem (39) can be given by

$$\begin{aligned}u(x,t)=&\sin(x)+\hbar t|\cos(x)|+(1+\hbar)u_1(x,t)\\&-\frac{t^2\hbar^2}{2!}\sin(x)+(1+\hbar)u_2(x,t)\\&+\frac{\hbar^3t^3}{3!}\,\mathrm{abs}(1,-\cos(x))\cos(x)\\&+\frac{(1+\hbar)\hbar t^2}{2!}\,\mathrm{abs}(1,\cos(x))\sin(x)+\ldots\end{aligned} \quad (51)$$

We have used the well-known software Maple 12 to compute the above relations. In this software the abs function denotes the first derivative of the absolute value function which is defined by

$$\mathrm{abs}(1,x)=\begin{cases}1, & \text{if } x>0,\\ 0, & \text{if } x=0,\\ -1, & \text{if } x<0.\end{cases}$$

By considering an appropriate interval for x and t, according to the change of sign of the $\sin(x)$ and $\cos(x)$ functions, and setting $\hbar=-1$ in (51) the solution of (39) can be obtained as the limit of one part of piecewise function $u=u_0+u_1+u_2+\ldots$. Thus the following formula which is the exact solution is obtained:

if $0\le t\le\frac{\pi}{2}$:

$$u(x,t)=\begin{cases}\sin(x-t), & \text{if } 0\le x\le\frac{\pi}{2},\\ \sin(x+t), & \text{if } \frac{\pi}{2}<x\le\frac{3\pi}{2}-t,\\ -1, & \text{if } \frac{3\pi}{2}-t<x\le\frac{3\pi}{2}+t,\\ \sin(x-t), & \text{if } \frac{3\pi}{2}+t<x\le 2\pi,\end{cases}$$

if $\frac{\pi}{2}\le t\le\pi$:

$$u(x,t)=\begin{cases}-1, & \text{if } 0\le x\le t-\frac{\pi}{2},\\ \sin(x-t), & \text{if } t-\frac{\pi}{2}<x\le\frac{\pi}{2},\\ \sin(x+t), & \text{if } \frac{\pi}{2}<x\le\frac{3\pi}{2}-t,\\ -1, & \text{if } \frac{3\pi}{2}-t<x\le 2\pi,\end{cases}$$

if $t\ge\pi$: $u(x,t)=0$.

4.3. Example 3

The third test problem is the initial value problem

$$u_t-(1+u_x^2)^{1/2}=0, \tag{52}$$

subject to the initial condition

$$u(x,0)=\begin{cases}1/2-x, & \text{if } x\le\frac{1}{2},\\ x-1/2, & \text{if } x>\frac{1}{2}.\end{cases} \tag{53}$$

The initial front 'V' is formed by rays meeting at (1/2,0). By entropy condition, the solution at any time t is the set of all points located a distance t from the initial 'V'. See [56] for details. Under the rule of solution expression and according to the initial condition (53), it is straightforward to choose

$$u_0(x,t)=u(x,0)=\begin{cases}1/2-x & \text{if } x\le\frac{1}{2},\\ x-1/2 & \text{if } x>\frac{1}{2},\end{cases} \tag{54}$$

and the auxiliary linear operator

$$\mathcal{L}[\phi(x,t;p)]=\frac{\partial\phi(x,t;p)}{\partial t} \tag{55}$$

with the property

$$\mathcal{L}(c)=0, \tag{56}$$

where c is the integral constant. In view of the HAM technique, we construct the zeroth-order deformation equation, with assumption $H(x,t)=1$, as follows:

$$(1-p)\mathcal{L}[\phi(x,t;p)-u_0(x,0)]=p\hbar\mathcal{N}(\phi(x,t;p)), \tag{57}$$

where

$$\mathcal{N}[\phi(x,t;p)]=\phi_t(x,t;p)-\sqrt{1+\phi_x^2(x,t;p)}. \tag{58}$$

Differentiating (57) m times with respect to p, then setting $p=0$ and finally dividing them by $m!$, we have the mth-order deformation equation

$$\mathcal{L}[u_m(x,t)-\chi_m u_{m-1}(x,t)]=\hbar\mathcal{R}_m(\vec{u}_{m-1}).$$

Accordingly, the first few terms of the HAM approximate solution can be shown by

$$u_m(x,t)=\chi_m u_{m-1}(x,t)+\hbar\mathcal{L}^{-1}[\mathcal{R}_m(\vec{u}_{m-1})]+c_1. \tag{59}$$

In accord with the initial condition, we have $u_m(\frac{1}{2},0)=0$ that implies $c_1=0$. The first few terms of HAM solution series are as given in the following:

$$\begin{aligned}
&u_0(x,t)=\begin{cases}1/2-x & \text{if } x\le\frac{1}{2},\\ x-1/2 & \text{if } x>\frac{1}{2},\end{cases}\\
&u_1(x,t)=-\sqrt{2}\hbar t,\quad x\neq\frac{1}{2},\\
&u_2(x,t)=(1+\hbar)u_1(x,t),\\
&u_3(x,t)=(1+\hbar)u_2(x,t)=(1+\hbar)^2u_1(x,t),\\
&u_4(x,t)=(1+\hbar)u_3(x,t)=(1+\hbar)^3u_1(x,t),\\
&\vdots
\end{aligned}$$

Hence, the HAM series solution of the initial-value problem (52) can be given by

$$\begin{aligned}
u(x,t)&=u_0(x,t)+u_1(x,t)+\sum_{m=2}^{\infty}u_m(x,t)\\
&=u_0(x,t)-\hbar t\sqrt{2}+u_1(x,t)\sum_{m=2}^{\infty}(1+\hbar)^{m-1}\\
&=u_1(x,t)\sum_{m=2}^{\infty}(1+\hbar)^{m-1}+\begin{cases}1/2-x+\sqrt{2}t, & \text{if } x\le\frac{1}{2},\\ x-1/2+\sqrt{2}t, & \text{if } x>\frac{1}{2}.\end{cases}
\end{aligned} \tag{60}$$

It is seen that the convergence results can be obtained when $-2 < \hbar < 0$. Now, by setting $\hbar = -1$ in (60), we have the following formula, which is the exact solution of problem (52)

$$u(x,t) = \begin{cases} 1/2 - x + \sqrt{2}t, & \text{if } x \le \frac{1}{2}, \\ x - 1/2 + \sqrt{2}t, & \text{if } x > \frac{1}{2}. \end{cases}$$

4.4. Example 4

As the last example we consider the following initial value problem which appears in the application of the model introduced in this paper in computer vision:

$$u_t + \mathcal{I}(x,y)\sqrt{u_x^2 + u_y^2 + 1} = 1 \tag{61}$$

with initial condition

$$u(x,y,0) = 0. \tag{62}$$

The steady state solution of this problem is the shape lighted by a source located at infinity with vertical direction. See [5] for details. We take

$$\mathcal{I}(x,y) = \frac{1}{\sqrt{1 + (1-|x|)^2 + (1-|y|)^2}},$$

the exact steady solution is

$$u(x,y,\infty) = (1-|x|)(1-|y|).$$

According to HAM, we choose the initial approximation

$$u_0(x,y,t) = u(x,y,0) = 0 \tag{63}$$

and the linear operator

$$\mathcal{L}[\phi(x,y,t;p)] = \frac{\partial \phi(x,y,t;p)}{\partial t} \tag{64}$$

with the property

$$\mathcal{L}(c) = 0, \tag{65}$$

where c is the integral constant. Furthermore, (62) suggests to define the nonlinear operator as

$$\begin{aligned} \mathcal{N}[\phi(x,y,t;p)] &= \phi_t(x,y,t;p) \\ &\quad + \mathcal{I}(x,y)\sqrt{\phi_x^2 + \phi_y^2 + 1} - 1. \end{aligned} \tag{66}$$

Using the above definition, with assumption $H(x,y,t) = 1$, we construct the zeroth-order deformation equation

$$(1-p)\mathcal{L}[\phi(x,y,t;p) - u_0(x,0)] = p\hbar\mathcal{N}(\phi(x,y,t;p)), \tag{67}$$

subject to the initial condition

$$u_m(0,0) = 0. \tag{68}$$

Then, the mth-order deformation equation is

$$\mathcal{L}[u_m(x,y,t) - \chi_m u_{m-1}(x,y,t)] = \hbar\mathcal{R}_m(\vec{u}_{m-1}). \tag{69}$$

Now the solution of mth-order deformation equation (61) for $m \ge 1$ becomes

$$\begin{aligned} &u_0(x,y,t) = 0, \\ &u_1(x,y,t) = (\mathcal{I}-1)\hbar t, \\ &u_2(x,y,t) = (1+\hbar)u_1(x,y,t) = (1+\hbar)\hbar t(\mathcal{I}-1), \\ &u_3(x,y,t) = (1+\hbar)u_2(x,y,t) + \frac{\hbar^3 \mathcal{I} t^3 f(x,y)}{3!}, \\ &\quad \text{where } f(x,y) = \frac{(1-|x|)^2 + (1-|y|)^2}{(1 + (1-|x|)^2 + (1-|y|)^2)^3}, \\ &\vdots \end{aligned}$$

So the approximate HAM series solution truncated in the fourth term is:

$$\begin{aligned} u(x,y,t) &\approx u_0 + u_1 + u_2 + u_3 \\ &= u_1(x,y,t) + (1+\hbar)u_1(x,y,t) \\ &\quad + (1+\hbar)^2 u_1(x,y,t) + \frac{\hbar^2 \mathcal{I} t^3 f(x,y)}{3!} \\ &= (1 + (1+\hbar) + (1+\hbar)^2)\hbar(\mathcal{I}-1)t \\ &\quad + \frac{\hbar^3 \mathcal{I} t^3 f(x,y)}{3!}. \end{aligned}$$

Note that this series contains the auxiliary parameter $\hbar$, which influences its convergence region and rate. We should therefore focus on the choice of $\hbar$ by plotting of $\hbar$-curve. Figure 1 shows the $\hbar$-curve of $u(0,0,0.08)$, $u(0.5,0.5,0.08)$, and $u(3,3,0.08)$ given by 4th-term approximate solution of (61). It is seen that convergence results can be obtained when $-2 < \hbar < 0$. To show the convergence behaviour of the approximate solution compared with the exact solution of this problem, in Tables 1–2 the values of $\|u - u_{\text{HAM}}\|_\infty$ for different values of $\hbar$ are listed. Also, the results in Tables 1–2 for $-2 < \hbar < 0$ confirm the validity of HAM

$dx = dy = 2/n$	t	$\hbar = -1$	$\hbar = -0.9$	$\hbar = -0.7$	$\hbar = -0.5$
40	0.02	4.1991×10^{-2}	4.1996×10^{-2}	4.2139×10^{-2}	4.2679×10^{-2}
	0.04	3.6482×10^{-2}	3.6493×10^{-2}	3.6779×10^{-2}	3.7858×10^{-2}
	0.06	3.0975×10^{-2}	3.0990×10^{-2}	3.1419×10^{-2}	3.3038×10^{-2}
	0.08	2.5470×10^{-2}	2.5490×10^{-2}	2.5490×10^{-2}	2.8218×10^{-2}
80	0.02	1.8693×10^{-2}	1.8698×10^{-2}	1.8846×10^{-2}	1.9403×10^{-2}
	0.04	1.3011×10^{-2}	1.3022×10^{-2}	1.3318×10^{-2}	1.4431×10^{-2}
	0.06	7.3314×10^{-3}	7.3476×10^{-3}	7.7895×10^{-3}	9.4594×10^{-3}
	0.08	4.2684×10^{-3}	4.2715×10^{-3}	4.4160×10^{-3}	5.0955×10^{-3}
160	0.02	6.5798×10^{-3}	6.5798×10^{-3}	6.7298×10^{-3}	7.2952×10^{-3}
	0.04	2.1399×10^{-3}	2.1423×10^{-3}	2.2142×10^{-3}	2.5531×10^{-3}
	0.06	4.9623×10^{-3}	4.9459×10^{-3}	4.4971×10^{-3}	2.8015×10^{-3}
	0.08	1.0707×10^{-2}	1.0707×10^{-2}	1.0110×10^{-2}	7.8495×10^{-3}

Table 1. Maximum absolute error between the exact solution (61) and the HAM solution for different values of $\hbar$.

$dx = dy = 2/n$	t	$\hbar = -1.1$	$\hbar = -1.3$	$\hbar = -1.6$	$\hbar = -1.9$
40	0.02	4.1985×10^{-2}	4.1842×10^{-2}	4.0801×10^{-2}	3.7975×10^{-2}
	0.04	3.6471×10^{-2}	3.6186×10^{-2}	3.4105×10^{-2}	2.8455×10^{-2}
	0.06	3.0959×10^{-2}	3.0533×10^{-2}	2.7415×10^{-2}	1.8945×10^{-2}
	0.08	2.5451×10^{-2}	2.4885×10^{-2}	2.0735×10^{-2}	1.0341×10^{-2}
80	0.02	1.8687×10^{-2}	1.8540×10^{-2}	1.7466×10^{-2}	1.4551×10^{-2}
	0.04	1.3000×10^{-2}	1.2706×10^{-2}	1.0560×10^{-2}	5.1927×10^{-3}
	0.06	7.3155×10^{-3}	6.8751×10^{-3}	4.8222×10^{-3}	5.0764×10^{-3}
	0.08	4.2658×10^{-3}	4.1394×10^{-3}	3.3940×10^{-3}	1.4870×10^{-3}
160	0.02	6.5684×10^{-3}	6.4185×10^{-3}	5.3282×10^{-3}	2.5993×10^{-3}
	0.04	2.1375×10^{-3}	2.0714×10^{-3}	1.6995×10^{-3}	7.6015×10^{-3}
	0.06	4.9785×10^{-3}	5.4580×10^{-3}	8.6911×10^{-3}	1.7502×10^{-2}
	0.08	1.0748×10^{-2}	1.1342×10^{-2}	1.8614×10^{-2}	2.7507×10^{-2}

Table 2. Maximum absolute error between the exact solution (61) and the HAM solution for different values of $\hbar$.

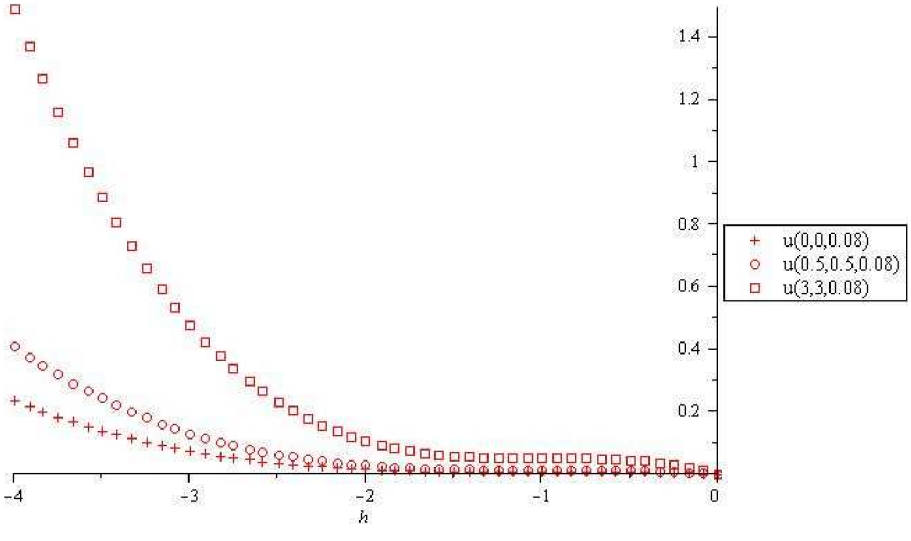

Fig. 1. $\hbar$-curve of 4th-term approximation of $u(0, 0, 0.08)$, $u(0.5,0.5,0.08)$, $u(3, 3, 0.08)$.

for the eikonal equation. The results for $\hbar = -1, H = 1$ are exactly the same as the results for homotopy perturbation method (HPM). Furthermore, the comparison between the results shows that the HPM results are not the optimal results in this case.

5. Applications

In this section we give some applications of the time-dependent partial differential eikonal equation.

5.1. Optimal Control

In this subsection we follow [1, 5] to prescribe an optimal control application of the studied model in this research. It is now well known, after the work of Crandall and Lions [57], that in some situations a viscosity solution may be considered as the cost function of an optimal control problem. We shall use here the formulation of $u(x)$ in terms of a value function and more precisely, the dynamic programming principle of Bellman.

Let $u(x,t)$ be the viscosity solution of (2). With the remark that [5]

$$|\nabla u(x)| = n(x) \Longleftrightarrow \sup\{\nabla u(x)\cdot q - n(x)\} = 0, \quad \forall x \in \Omega, \tag{70}$$

$u(x)$ appears to be the cost function of the following exit time problem, which is the Hamilton-Jacobi-Bellman equation of a minimum time problem for dynamical systems [1]: let y_x be the state of the controlled dynamical system,

$$\begin{aligned} &\dot{y}_x = -q(s), \quad s \geq 0, \\ &y_x(0) = x, \end{aligned} \tag{71}$$

where q, the control, belongs to

$$\mathcal{A} = \{q : \mathbb{R}_+ \longrightarrow \mathbb{R}^2 \ \text{ measurable } \mid |q(s)| \leq 1, s \geq 0\}. \tag{72}$$

Here the problem is to minimize a finite horizon cost function which is defined by [5]:

$$\mathcal{J}(x, q(,)) = \int_0^T n(y_x(s))\mathrm{d}s + \phi(y_x(T)), \tag{73}$$

where T denotes the first exit time of Ω, i. e., $T = \min\{t \geq 0 \mid y_x(t) \in \partial\Omega\}$.

The dynamic programming method suggests that the cost function

$$u(x,t) := \inf \mathcal{J}(x, q(,)) \tag{74}$$

of the finite horizon problem solves, for all $T > 0$,

$$\begin{aligned} &u_t(x,t) + H(x, D_x u(x,t)) = 0, \ \text{ in } \mathbb{R}^N \times (0,T), \\ &u(x,0) = \phi(x), \qquad\qquad\quad \text{in } \mathbb{R}^N, \end{aligned} \tag{75}$$

where the Hamiltonian is $H(x,p) := \sup_{|q|\leq 1}\{p\cdot q - n(x)\}$.

5.2. Halftoning

In this subsection we follow [58, 59] to prescribe an application of the studied model in halftoning. A halftone is a binary picture $H(x,y)$, each point being either completely black or completely white that gives the impression of an image containing shads of grey. Halftoning is the process of transforming a grey-level image, $f(x,y)$, into a halftone, with the aim that when $H(x,y)$ is displayed on a bilevel medium, the human observer will see in it as a good approximation as possible of the original $f(x,y)$ [59]. One way to mathematically translate the halftone paradigm into a live generation algorithm is via the eikonal equation.

In the rest of this section we follow [58, 59] to show that the equal height lines of the solution $H(x,y)$ of the eikonal equation obey the halftone paradigm. Then, we follow [21] to introduce a time-dependent formulation of the eikonal equation by the level set method which can be solved by the method presented in this report.

Suppose we want to determine a bivariate function $H(x,y)$, so that the local density of its equal height contours (level sets) corresponding to the equally spaced levels, defined by $\{H(x,y) = nh \mid n \in \mathbb{Z}\}$, will be proportional to a given image $f(x,y) > 0$. Assuming that in the neighbourhood of a point (x_0, y_0) the bivariate function can be approximated by a planner patch, that can be written as

$$\begin{aligned} H(x,y) = H(x_0,y_0) &+ p(x_0,y_0)(x-x_0) \\ &+ q(x_0,y_0)(y-y_0), \end{aligned}$$

where p and q are the partial derivatives of $H(x,y)$, with respect to the x and y-coordinates [59]. In the neighbourhood of (x_0,y_0), the level sets corresponding to nh are equally spaced parallel lines, separated by a distance d, which is given by

$$d[p^2(x_0,y_0) + q^2(x_0,y_0)]^{1/2} = h.$$

The 'local density' of the parallel lines is proportional to the inverse of d [58], thus we need to have

$$[p^2(x_0,y_0) + q^2(x_0,y_0)]^{1/2} = \frac{h}{d} = f(x,y).$$

This shows that a solution of the partial differential equation

$$\left[\left(\frac{\partial H(x,y)}{\partial x}\right)^2 + \left(\frac{\partial H(x,y)}{\partial y}\right)^2\right]^{1/2} = f(x,y)$$

will yield a bivariate function $H(x,y)$ obeying the desired halftone paradigm.

Now by the method given in [21], (71) becomes

$$\upsilon_t + g|\nabla\upsilon| = 0,$$

where $g = \frac{-1}{f}$. Then to compute $H(x,y)$, we calculate the level set via the relation

$$\upsilon(x,t) = 0 \Longleftrightarrow t = H(x,y).$$

5.3. Shape Offset

In this subsection we follow [60, 61] to prescribe an application of the studied equation in computer aided design (CAD). In CAD one often encounters the need to find the offsets of a given curve. The problem of shape-offsetting is straightforward; it gives a closed shape in two or three dimensions and computes the offsets that are obtained by propagating the boundary in its normal direction with constant unit speed. The propagation time represents the 'offset distance' from the given curve. The problem of shape offsetting can be formulated as follows [60]: given a simple, closed planner curve

$$X_0(s) = [x(s), y(s)]^T,$$

where s is an arbitrary curve parameterization. Finding an offset curve is almost everywhere given by

$$X_L(s) = X_0(s) + \mathcal{N}(s,0)L,$$

where L is the displacement of the offset curve and $\mathcal{N}(s,0)$ is the unit normal at the point $X_0(s)$ given by

$$\mathcal{N}(s,0) = \frac{1}{(x_s^2(s) + y_s^2(s))}[-y_s(s), x_s(s)]^T.$$

Consider $X(s,t)$ to be a curve continuously changing in time, for all t, $X(s,t) = X_0(s) + t\mathcal{N}(s,0)$. Thus the curve evolution can be described differentially by

$$\frac{\partial X(s,t)}{\partial t} = \mathcal{N}(s,0), \quad X(s,0) = X_0(s),$$

or equivalently

$$\frac{\partial X(s,t)}{\partial t} = \mathcal{N}(s,t), \quad X(s,t) = X_0(s), \tag{76}$$

provided that each point on the curve moves in the direction of the instantaneous normal

$$\mathcal{N}(s,t) = [-y_s(s,t), x_s(s,t)]^T \frac{1}{(x_s^2(s,t) + y_s^2(s,t))}.$$

In [60], Kimmel and Bruckstein introduced an Eulerian scheme for curve propagation. The Eulerian framework is a recursive procedure which propagates the curve while inherently implementing the entropy condition. Authors of [60] introduced a smooth function $\phi(x,y,t)$ which is arbitrary initialized so that $\phi(x,y,0) = 0$ yields the curve $X(s,0)$ provided that ϕ is negative in the interior and positive in the exterior of the level set $\phi(x,y,0) = 0$. The idea is to determine an evolution of the surface $\phi(x,y,t)$ so that the level sets $\phi(x,y,0) = 0$ provide the curve $X(s,t)$ as if propagating by (76) and obeying the entropy condition. If $\phi(x,y,t) = 0$ along $X(s,t)$ then, by the chain rule, we have

$$\frac{\partial\phi(x,y,t)}{\partial t} + \frac{\partial\phi(x(s,t),y(s,t),t)}{\partial x}x_t + \frac{\partial\phi(x(s,t),y(s,t),t)}{\partial t}y_t = 0$$

or

$$\phi_t + X_t(s,t)\nabla\phi = 0. \tag{77}$$

The scaler velocity of each curve point in its normal direction is

$$\upsilon = \mathcal{N}(s,t)\cdot X_t(s,t).$$

In this case, we need to impose $\upsilon = 1$. The gradient $\nabla\phi$ is always normal to the curve given by $\phi(x,y,t) = 0$ [60] so that

$$\mathcal{N}(s,t) = -\frac{\nabla\phi}{|\nabla\phi|}$$

and hence

$$\upsilon = \mathcal{N}(s,t)\cdot X_t(s,t) = -\frac{\nabla\phi}{|\nabla\phi|}X_t(s,t) = 1. \tag{78}$$

Substituting (78) into (77) yields the surface evolution equation

$$\phi_t - |\nabla\phi| = 0,$$

which is the time-dependent eikonal equation and can be solved by the method introduced in this research.

5.4. Porous Medium

In this subsection we follow [62, 63] to prescribe a porous medium application of the model studied in this research. The porous medium equation arises in several areas such as percolation of gas through porous medium, radiative heat transfer in ionized plasma, etc.

Now, consider the following partial differential equations [63]:

$$\begin{aligned} &u_t = \Delta(u^m), \quad \text{in } \mathbb{R}^n \times (0, T_m), \\ &u(x,0) = u_0, \ \text{in } \mathbb{R}^n \times \{t = 0\}, \end{aligned} \tag{79}$$

and

$$\begin{aligned} &\upsilon_t = |\nabla \upsilon|^2, \ \text{in } \mathbb{R}^n \times (0, T_m), \\ &\upsilon = \upsilon_0, \qquad \text{in } \mathbb{R}^n \times \{t = 0\}, \end{aligned} \tag{80}$$

as the first is the porous medium equation and the second one is the eikonal equation. The connection between these equations is made apparent when we perform the change of variables

$$\upsilon = \frac{m}{m-1} u^{m-1},$$

which transforms (79) into the 'pressure' equation

$$\begin{aligned} &\upsilon_{mt} = (m-1)\upsilon_m \Delta \upsilon_m + |\nabla \upsilon|^2, \text{ in } \mathbb{R}^n \times (0, T_m), \\ &\upsilon_m = \upsilon_{m0}, \qquad\qquad\qquad \text{in } \mathbb{R}^n \times \{t = 0\}, \end{aligned} \tag{81}$$

letting $m \to 1$, then we obtain (80).

In [62], authors explored the convergence, as $m \to 1$, of the solution of (81) to (80) in the case of the Cauchy problem in one space dimension. They proved not only the solutions but also the interfaces of the solution (81) converge to the solution and the interfaces of (80), if the initial data is continuous, non-negative, and convergent locally uniformly. Also, in [63], authors showed the convergence behaviour in N space dimensions with general initial data both for the Cauchy problem in $\mathbb{R}^N$ and for the Dirichlet problem in a bounded domain in $\mathbb{R}^N$. They proved that the solution of (81) converge to the viscosity solution of (80). Moreover, they showed that the positivity sets of solutions of (81) converge to the positivity solution of (80) by means of introducing a new type estimates for the gradient.

6. Conclusions

In the current paper the homotopy analysis method is applied to find the exact and approximate solutions of a class of nonlinear Hamilton-Jacobi equations, namely the eikonal equations. The problem was formulated in time-dependent form by the aid of the level set method. This analytic approach has some obvious advantages. First of all, unlike perturbation techniques, it is independent of any small parameters: it is valid no matter whether or not there exist any small physical parameters in governing equations and/or boundary conditions. Secondly, this approach can be applied to solve partial differential problems with strong nonlinearity. Thirdly, unlike all other analytic techniques, this approach provides us great freedom to choose an auxiliary linear operator. This technique was tested on some examples and was seen to give satisfactory results. The results show that the homotopy analysis method logically contains the homotopy perturbation method when $\hbar = -1$ and a comparison between results reveals that the HPM outputs are not the optimal results in the case of the eikonal equation. However, the HAM provides us with a convenient way to control the convergence of approximation series, which is a fundamental qualitative difference in analysis between the HAM and other methods. This method provides the solution of the problem in a closed form while the mesh point techniques [64] provide the approximation at mesh points only. Moreover, since the new method does not need discretization of the variables, there is no computation round off errors and one is not faced with necessity of large computer memory and time.

Acknowledgements

The authors are very grateful to four reviewers for reading this paper and for their comments.

[1] M. Bardi and F. Dalio, Nonlinear Diff. Eqs. Appl. **4**, 491 (1997).
[2] M. Boue and P. Dupuis, SIAM J. Numer. Anal. **36**, 667 (1992).
[3] A. R. Bruss, J. Math. Phys. **23**, 890 (1982).
[4] P. Danielsson, Comput. Graphic Image Processing **14**, 227 (1980).
[5] E. Rouy and A. Tourin, SIAM J. Numer. Anal. **29**, 867 (1992).
[6] B. Engquist and O. Runborg, J. Comput. Appl. Math. **74**, 175 (1996).
[7] R. Kimmel and J. A. Sethian, J. Math. Imaging Vision **14**, 237 (2001).
[8] I. M. Mitchell and S. Sastry, IEEE **5**, 5502 (2003).
[9] W. K. Jeong and R. Whitaker, SIAM J. Sci. Comput. **30**, 2512 (2008).
[10] J. N. Tsitsiklis, IEEE Trans. Automatic Control **40**, 1528 (1995).
[11] Y. T. Zhang, H. K. Zhao, and J. Qian, J. Sci. Comput. **29**, 25 (2006).
[12] H. K. Zhao, Math. Comput. **74**, 603 (2005).

[13] S. Osher and C. W. Shu, SIAM J. Numer. Anal. **28**, 907 (1991).
[14] G. S. Jiang and D. P. Peng, SIAM J. Sci. Comput. **21**, 2126 (2000).
[15] F. Li, C. W. Shu, Y. T. Zhao, and H. Zhao, J. Comput. Phys. **227**, 8191 (2008).
[16] T. Cecil, J. Qian, and S. Osher, J. Comput. Phys. **196**, 327 (2004).
[17] L. T. Cheng and Y. H. Tsai, J. Comput. Phys. **227**, 4002 (2008).
[18] Y. T. Zhang and C. W. Shu, SIAM J. Sci. Comput. **24**, 1005 (2003).
[19] S. Osher and J. Sethian, J. Comput. Phys. **79**, 12 (1988).
[20] J. A. Sethian, Level set methods: evolving interface in geometry, fluid mechanics, computer vision, and material science, Cambridge University Press, Cambridge 1996.
[21] S. Osher, SIAM J. Math. Anal. **24**, 1145 (1993).
[22] B. Cockburn, J. Qian, F. Reitich, and J. Wang, J. Comput. Phys. **208**, 175 (2005).
[23] M. Dehghan and R. Salehi, Numer. Methods Part. Diff. Eqs. **26**, 702 (2010).
[24] S. J. Liao, On the proposed homotopy analysis technique for nonlinear problems and its applications, Ph.D. dissertation, Shanghai Jio Tong University, Shanghai 1992.
[25] S. J. Liao, Int. J. Nonlinear Mech. **32**, 815 (1997).
[26] S. J. Liao, Int. J. Nonlinear Mech. **34**, 759 (1999).
[27] S. J. Liao, Commun. Nonlinear Sci. Numer. Simul. **4**, 104 (1999).
[28] C. Wang, S. J. Liao, and J. Zhu, Int. J. Heat Mass Transf. **46**, 4813 (2003).
[29] M. Ayub, A. Rasheed, and T. Hayat, Int. J. Engin. Sci. **41**, 2091 (2003).
[30] H. Xu and J. Cang, Phys. Lett. A **372**, 1250 (2008).
[31] S. J. Liao, Appl. Math. Comput. **144**, 495 (2003).
[32] S. Abbasbandy, Chaos, Solitons, and Fractals **39**, 428 (2009).
[33] M. Inc, Phys. Lett. A **365**, 412 (2007).
[34] Y. Tan, H. Xu, and S. J. Liao, Chaos, Solitons, and Fractals **31**, 462 (2007).
[35] T. Hayat and Z. Abbas, Chaos, Solitons, and Fractals **38**, 556 (2008).
[36] S. Abbasbandy, Y. Tan, and S. J. Liao, Appl. Math. Comput. **188**, 1794 (2007).
[37] H. Jafari, M. Saeidy, and M. A. Firoozjaee, Numer. Methods Part. Diff. Eqs. DOI 10.1002/num.
[38] T. Hayat and M. Sajid, Int. J. Eng. Sci. **45**, 393 (2007).
[39] A. S. Bataineh and M. S. M. Noorani, Nonlinear Sci. Numer. Simul. **14**, 409 (2009).
[40] S. Abbasbandy, Z. Angew. Math. Phys. **59**, 51 (2008).
[41] M. Dehghan, J. Manafian, and A. Saadatmandi, Numer. Methods Part. Diff. Eqs. **26**, 448 (2010).
[42] M. Khan and S. Wang, Nonlinear Anal.: Real World Appl. **10**, 203 (2009).
[43] M. Khan, S. Hyder Ali, and H. Qi, Nonlinear Anal.: Real World Appl. **10**, 980 (2009).
[44] M. Khan, T. Hayat, and S. Asghar, Int. J. Eng. Sci **44**, 333 (2006).
[45] M. Khan, J. Porous Med. **12**, 919 (2009).
[46] F. Shakeri and M. Dehghan, Math. Comput. Modelling **48**, 486 (2008).
[47] M. Dehghan and F. Shakeri, Physica Scripta **78**, 1 (2008).
[48] M. Dehghan and F. Shakeri, New Astron. **13**, 53 (2008).
[49] M. Tatari and M. Dehghan, J. Comput. Appl. Math. **207**, 201 (2007).
[50] M. Dehghan and R. Salehi, Comput. Phys. Commun. **181**, 1255 (2010).
[51] M. Dehghan, M. Shakourifar, and A. Hamidi, Chaos, Solitons, and Fractals **39**, 2509 (2009).
[52] A. Saadatmandi and M. Dehghan, Comput. Math. Appl. **58**, 2190 (2009).
[53] A. Ghorbani, Chaos Solitons, and Fractals **39**, 1486 (2009).
[54] Y. Cheng and C. W. Shu, J. Comput. Phys. **223**, 398 (2007).
[55] C. Hu and C. W. Shu, SIAM J. Sci. Comput. **21**, 666 (1999).
[56] J. A. Sethian, Theory, algorithms, and applications of level set methods for propagating interfaces, Acta Numerica, Cambridge University Press, Cambridge 1996.
[57] M. G. Crandall and P. L. Lions, Trans. Amer. Math. Soc. **227**, 1 (1983).
[58] A. C. Bouik and A. Bouik, Handbook of image and video processing, Academic Press, New York 2005.
[59] Y. Pnueli and A. M. Bruckstein, Graphic models Image Process. **58**, 38 (1996).
[60] R. Kimmel and A. M. Bruckstein, CAD **25**, 154 (1993).
[61] R. Kimmel, Curve evolution on surfaces, Ph. D. dissertation, Technion Israel Institute of Technology, 1995.
[62] D. G. Arenson and L. A. Caffarelli, Rev. Mat. Iberoamericana **2**, 357 (1986).
[63] P. L. Lions, P. E. Souganidis, and J. L. Vazquez, Rev. Mat. Iberoamericana **3**, 275 (1987).
[64] M. Dehghan, Math. Comput. Simul. **71**, 16 (2006).
[65] M. Dehghan and M. Tatari, Int. J. Comput. Math. **87**, 1256 (2010).
[66] S. A. Yousefi and M. Dehghan, Int. J. Comput. Math. **87**, 1299 (2010).
[67] M. Dehghan and M. Shakeri, Int. J. Numer. Meth. Biomed. Eng. **26**, 705 (2010).
[68] M. Dehghan, J. Manafian, and A. Saadatmandi, Math. Appl. Sci. **33**, 1384 (2010).
[69] A. Saadatmandi, M. Dehghan, and A. Eftekhari, Nonlinear Anal.: Real Word Appl. **10**, 1912 (2009).